Communication: Fullerene resolution by the magnetic circular dichroism

Petr Štěpánek,[1,2] Michal Straka,[1] Valery Andrushchenko,[1] and Petr Bouř[1,a)]

[1]*Institute of Organic Chemistry and Biochemistry, Academy of Sciences, Flemingovo náměstí 2, 16610 Prague, Czech Republic*
[2]*Faculty of Mathematics and Physics, Charles University, Ke Karlovu 5, 121 16 Prague, Czech Republic*

The similarity in shape makes separation and identification of fullerenes difficult. In this work, the magnetic circular dichroism (MCD) spectroscopy is presented as a useful tool for this purpose. Experimental C_{60} and C_{70} spectra were obtained and reproduced with the aid of density functional computations and the complex polarization propagator method. Theoretical spectra of other fullerenes revealed distinctive patterns extremely sensitive to molecular structure as well. Requiring tiny amounts of the sample, the MCD technique thus appears as a useful for detailed fullerene studies. © *2013 AIP Publishing LLC.* [http://dx.doi.org/10.1063/1.4802763]

The fullerene discovery belongs to triumphs of preparation chemistry.[1] These molecules are nowadays considered for many applications including hydrogen storage, molecular devices, photovoltaic systems, magnetic resonance imaging agents, and quantum computing.[2–10] Typically, high performance liquid chromatography (HPLC) coupled with ^{13}C nuclear magnetic resonance (NMR) or mass spectrometry is used for their analysis.[11–14]

However, their discrimination is complicated due to their similar physical properties. Fullerene shapes are close to a sphere or ellipsoid, and often exhibit a high degree of symmetry. The buckminsterfullerene C_{60} itself belongs to the I_h point group comprising 120 symmetry elements. Larger fullerenes of a single stoichiometric formula can exist in many forms. For example, C_{84} can generate 24 isomers, about half of which have been observed experimentally.[15] For C_{100}, 450 possible isomers have been predicted by the spiral algorithm.[16]

The magnetic circular dichroism (MCD) spectroscopy can be helpful in this process as it provides extensive information about electronic and molecular structure. It measures the difference in absorption of left- and right-circularly polarized light in the presence of magnetic field. The measurement is generally available by extension of common dichrographs by a magnet. Molecular MCD is traditionally decomposed to three terms, A, B, and C.[17,18] The C term is exhibited by open-shell systems only. The B term (positive or negative) is the most common as it is always present. It originates from mixing of molecular electronic states under influence of the magnetic field. Highly symmetric structures with degenerate orbitals also support the A term producing a couplet. Fullerenes, therefore, provide many transitions active in the spectra, and these significantly differ according to molecular structure.

The signs of spectral bands and other spectral features conveniently complement the absorption spectroscopy, also successfully used for fullerene characterization.[19,20] Unlike ^{13}C NMR, the MCD spectroscopy requires a significantly smaller amount of sample (6–37 μg dissolved in a milliliter for our experiments).

Early MCD C_{60} spectra were collected in argon matrices[21] and interpreted using semiempirical calculations.[22] Fine vibrational structure of the bands was also analyzed.[23,24] An interesting MCD counterpart is the magnetic vibrational circular dichroism, for C_{60} revealing behavior of its vibrational states.[25]

A new interest in MCD has been boosted by accurate density functional theory (DFT) computations.[26–32] These are possible, for example, within the DALTON[33] and ADF[34] program suites. Recently, simulated cyanocobalamin or porphyrin are typical systems approachable by such computational methodology.[35–37]

In spite of the fullerene size, we could calculate the MCD spectra with reasonable accuracy by the complex polarization propagator method[32] as implemented in the DALTON program. The computations are compared to experimental spectra obtained for *n*-hexane solutions at room temperature.

As a test case, C_{60} and C_{70} fullerene absorption and MCD spectra within 200–420 nm for C_{60} and 215–700 nm for C_{70} were measured using a Jasco J-815 spectrometer equipped with 1.5 T permanent magnet. The presented absorption spectra were measured on a different, double-beam Varian Cary 5000 UV-Vis-NIR spectrophotometer that allowed for a more precise absorption measurement. C_{60} solution in *n*-hexane was prepared at concentration of 37 μg/ml (for the measurements within 300–420 nm) and diluted 4 times (for 300–400 nm), 8 times (for 280–300 nm), and 16 times (for 200–280 nm). The C_{70} concentration was 13 μg/ml for 300–700 nm and 6.5 μg/ml for 215–300 nm. Different sample concentrations were required due to large differences in the absorption throughout the spectrum. The highest concentrations correspond to the saturated solutions.[38,39] The solvent spectra were subtracted from the sample solution spectra. The MCD spectra were obtained at both orientations of the magnet in order to distinguish real transitions from baseline artifacts (see Figure S1 in the supplementary material[40]).

Spectral simulations were based on fullerene geometries obtained by energy minimization at the RI-BP86[41,42] level

---

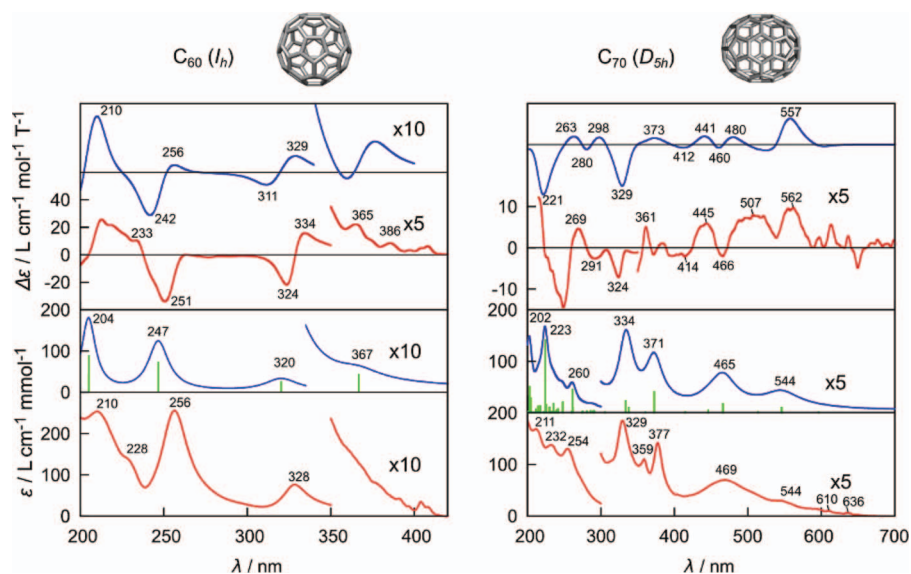a)Electronic mail: bour@uochb.cas.cz. Tel.: (+420) 220 183 348. Fax: (+420) 220 183 578.

FIG. 1. Calculated (blue upper, B3LYP/6-31G*) and experimental (red, lower) MCD ($\Delta\varepsilon$) and absorption (ε) spectra of C_{60} and C_{70}. Line positions and intensities are indicated for calculated absorption in green. The experimental MCD below 240 nm is somewhat less reliable due to the high total absorption.

using the Turbomole 6.3.1[43] program. Alternate usage of the B3LYP[41]/6-31G* geometry led to very similar spectra (Figure S2 in the supplementary material[40]). The absorption spectra were calculated using the B3LYP functional and 6-31G, 6-31G*, and 6-31+G* basis sets in the Turbomole program. We have chosen B3LYP as it usually performs well for valence-excited states, which is the nature of lowest-lying excited states in fullerenes.[44] Performance of other functionals was also tested (Figure S3 in the supplementary material[40]). The number of excited electronic states was limited to cover the experimentally accessible region ($\sim$200–800 nm). Solvent and basis set variations were tested (for C_{70}, see Figure S4 in the supplementary material[40]), and had a rather limited influence on the spectra.

MCD spectra were calculated using the complex polarization propagator (CPP),[32] B3LYP functional, and 6-31G* basis set as implemented in the DALTON[33] program. Within the CPP approach the band shapes are directly calculated with a finite width, which was controlled by a damping parameter varied linearly from 0.2 eV at 200 nm to 0.04 eV at 700 nm. This progression corresponded to the experiment, where the bandwidths are approximately uniform in the wavelength scale.

As can be seen in Figure 1, both the C_{60} and C_{70} molecules provide distinct absorption and MCD spectral patterns. C_{60} exhibits a very low absorption threshold ($\sim$350 nm), and relatively simple MCD pattern. Positive and negative intensities are rather balanced; the signal is largely composed of close positive and negative bands of similar magnitudes ("couplets"). At the longest-wavelength region a weak positive sign prevails. Very weak transitions with longer wavelengths are also visible in the experimental absorption spectra (see details of the electronic structure in Tables S1–S3 in the supplementary material[40]). The balanced character of MCD (e.g., the couplet at 324/334 nm) reflects the high symmetry of the molecule, which favors A term-originated bands. The symmetry of C_{70} is lower (D_{5h}), and the spec-

trum is richer and less balanced, most probably with a significant contribution of B terms (which cannot be calculated separately within the CPP approach) in a wider interval of wavelengths. The lower symmetry in C_{70} causes more transitions to be electric dipole-allowed, which results in a more complex absorption spectrum as well.

The computations reproduce most of the experimental MCD features. For C_{60}, the theory suggests four couplets centered at 367, 320, 247, and 204 nm as the primary source of the intensity. Due to the adopted broadening, the negative band of the 366 nm transition is overlapped with the positive lobe of the 320 nm couplet. The longest-wavelength region is known to exhibit some vibrational structure[21, 24] visible also in our experimental spectrum, e.g., the positive MCD band at 386 nm.

The simulated MCD is also in agreement with a recent computation based on real-time time-dependent DFT.[45] The real-time method based provided couplets approximately at the same positions but more balanced than in our simulations. Although currently less accurate than static approaches, the real-time simulations are promising especially for highly symmetric molecules and high-energetic excitations.[45, 46] High symmetry molecules can also be treated by the sum over state approach that we applied recently[47] for the C_{60} molecule obtaining spectra of similar quality as the complex polarization method used in the present study.

For C_{70}, the minor MCD features above 600 nm are not reproduced by the calculation, and the calculated negative signal around 520 nm does not fully appear in experiment. Overall, however, as for C_{60}, the calculation reproduces the absorption and MCD spectra with a reasonable accuracy and resolution. The overall good performance of the computations can be attributed to the low polarity of the fullerenes, consequent small solvent effects, and the exclusive presence of carbon atoms in the molecule.

To investigate the possibilities of fullerene MCD identification further, we calculated the MCD and absorption spectra
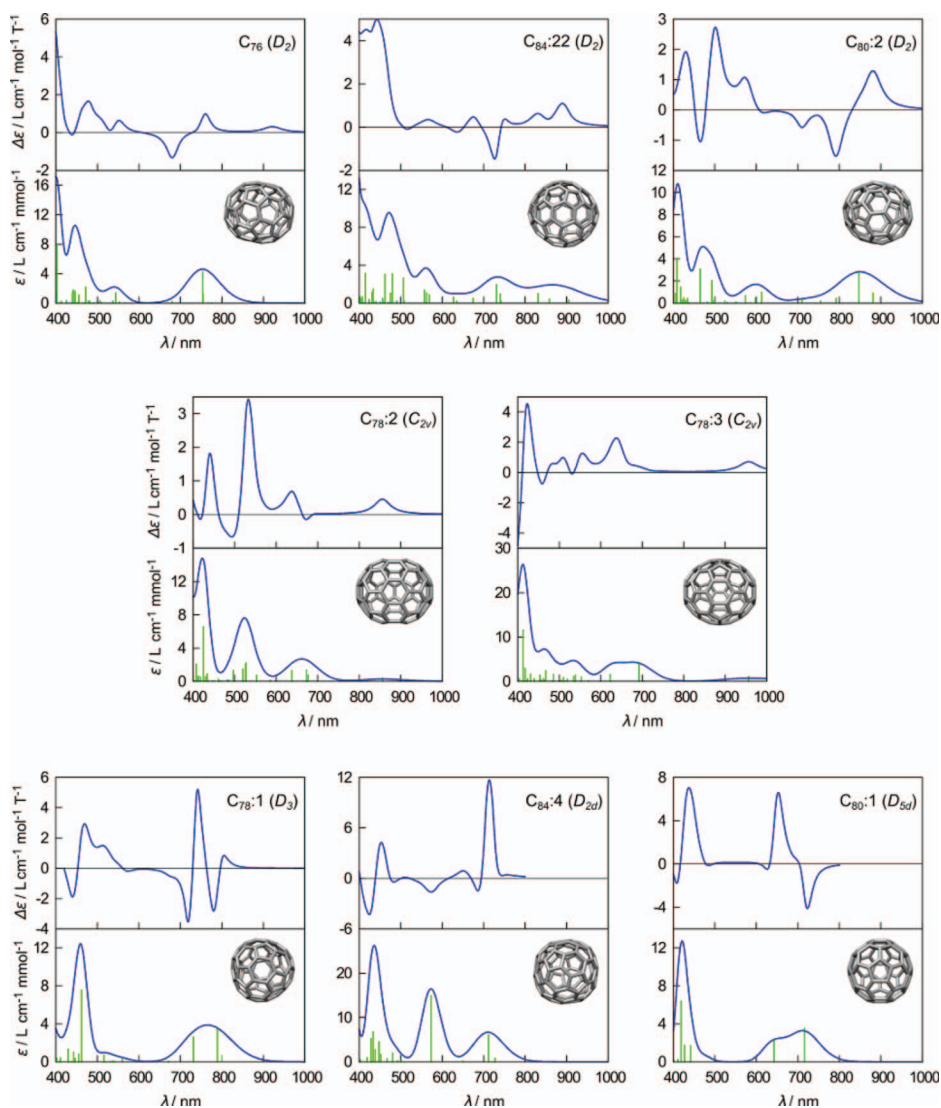
FIG. 2. MCD and absorption spectra of a series of fullerenes calculated at the B3LYP/6-31G* approximation level.

of a series of molecules, C_{76}:1 (D_2), C_{84}:22 (D_2), C_{80}:2 (D_2), C_{78}:2 (C_{2v}), C_{78}:3 (C_{2v}), C_{78}:1 (D_3), C_{84}:4 (D_{2d}), and C_{80}:1 (D_{5d}). Here, we use the convention of the isomer number after the colon, with symmetry in parentheses. The computations reveal that the absorption and MCD patterns are quite unique for each system (Figure 2). For example, there are clear differences in signs and relative band intensities even in MCD spectra of two isomers of the same C_{78} formula and symmetry (C_{2v}), isomers 2 and 3. Within 500–800 nm where both the C_{2v} symmetric forms of C_{78} provide predominantly positive MCD, a more complicated w-shaped character is observed for the C_{78}:1 (D_3) isomer. The more sign-balanced MCD of the latter corresponds to the dominance of the A terms.

MCD spectra of the fullerenes with D_2 symmetry (C_{76}:1, C_{84}:22, C_{80}:2, upper part of Figure 2) somewhat resemble each other, having a negative signal around 700–800 nm, and a predominantly positive one in the neighboring wavenumber regions. Nevertheless, their detailed MCD features are quite specific, as are the spectra of fullerenes of higher symmetries (C_{84}:22 (D_{2d}) and C_{80}:1 (D_{5d}), lower part of Figure 2). Interestingly, both the absorption and MCD spectra of the C_{80}:1

molecule with a high symmetry (D_{5d}) are rather simple, with two positively biased MCD couplets centered around absorption bands at ∼420 and 700 nm, which reminds the spectral behavior of C_{60}. Note that, similarly as C_{60} (I_h), fullerenes with one or more 3-fold or higher symmetry axes, such as C_{80}:1(D_{5d}) and C_{78}:1(D_3) support the MCD A terms. This feature is manifested by a more balanced MCD pattern, as seen from the comparison with the spectra of lower symmetry species.

Orbital energies and shapes (Figure S5)[40] provide a different representation of the electronic structure reflected in the spectra. For example, the C_{78}:2 and C_{78}:3 isomers have visually very similar HOMO (a2) and LUMO (b2) orbitals. However, the orbital energies and, hence, the HOMO-LUMO gap are markedly different for these species. The larger gap in C_{78}:2 isomer is reflected in the lower-wavelength onset of absorption for this isomer (∼850 nm, Figure 2) than for C_{78}:3 (∼950 nm). The D_3 symmetry isomer of C_{78}:1 has both different orbital shapes and energies if compared to the C_{2v} isomers. In Figure 2 we saw that it also had rather different MCD spectra with A term

features. Similarly, despite some common features of the spectra, the relative orbital energies of C_{80}:2 and C_{84}:22, both D_2, are markedly different. For example, the order of LUMO and LUMO+1 is switched with respect to their symmetries (a and b_2).

Obviously, future experimental tests are needed to test the extent to which MCD is applicable to fullerene discrimination. The computations suggest that the technique is universal in providing more information than the absorption; however, applications to symmetric fullerenes with a few spectral features only may be more problematic than for lower-symmetry species. An accuracy improvement of the theory to reproduce fine spectral differences is desirable. Our and previous experiments also reveal a relatively rich vibrational structure of the longest-wavelength (lowest-energy) bands, which can both obscure the interpretation of spectral patterns, or if reproducible provide additional information about the structure.

In summary, the results indicate that fullerenes of similar structure provide very distinct MCD spectral patterns. The MCD spectroscopy coupled with the computations thus represents a powerful tool for identification of different fullerenes and their isomers as well as for providing insight into their electronic structure. Although improvements in speed and accuracy of the computations are desirable, the main predicted features appear quite reliable. The experimental spectra of C_{60} and C_{70} agreed well with the theoretical predictions, and documented the sensitivity of the technique requiring microgram amounts of fullerenes.

[1]H. W. Kroto, J. R. Heath, S. C. O'Brien, R. F. Curl, and R. E. Smalley, Nature (London) **318**, 162–163 (1985).
[2]L. Türker, Int. J. Hydrogen Energy **28**, 1115–1119 (2003).
[3]J. J. L. Morton, A. Tiwari, G. Dantelle, K. Porfyrakis, A. Ardavan, and G. A. D. Briggs, Phys. Rev. Lett. **101**, 013002 (2008).
[4]T. Huang, J. Zhao, M. Feng, A. A. Popov, S. Yang, L. Dunsch, and H. Petek, Nano. Lett. **11**, 5327–5332 (2011).
[5]R. B. Ross, C. M. Cardona, D. M. Guldi, S. G. Sankaranarayanan, M. O. Reese, N. Kopidakis, J. Peet, B. Walker, G. C. Bazan, E. Van Keuren, B. C. Holloway, and M. Drees, Nature Mater. **8**, 208–212 (2009).
[6]K. Sawai, Y. Takano, M. Izquierdo, S. Filippone, N. Martin, Z. Slanina, N. Mizorogi, M. Waelchli, T. Tsuchiya, T. Akasaka, and S. Nagase, J. Am. Chem. Soc. **133**, 17746–17752 (2011).
[7]C. Ju, D. Suter, and J. Du, Phys. Lett. A **375**, 1441–1444 (2011).
[8]L. Dunsch and S. Yang, Phys. Chem. Chem. Phys. **9**, 3067–3081 (2007).
[9]X. Lu, L. Feng, T. Akasaka, and S. Nagase, Chem. Soc. Rev. **41**, 7723–7760 (2012).
[10]A. Rodriguez-Fortea, A. L. Balch, and J. M. Poblet, Chem. Soc. Rev. **40**, 3551–3563 (2011).
[11]T. Lyu, L. Shiu, T. Luh, and G. Her, Rapid Commun. Mass Spectrom. **9**, 93–96 (1995).
[12]T. J. S. Dennis, T. Kai, K. Asato, T. Tomiyama, H. Shinohara, T. Yoshida, Y. Kobayashi, H. Ishiwatari, Y. Miyake, K. Kikuchi, and Y. Achiba, J. Phys. Chem. A **103**, 8747–8752 (1999).
[13]N. Tagmatarchis, A. G. Avent, K. Prassides, T. J. S. Dennis, and H. Shinohara, Chem. Commun. **1999**, 1023–1024.
[14]T. J. S. Dennis, T. Kai, T. Tomiyama, and H. Shinohara, Chem. Commun. **1998**, 619–620.
[15]B. Ahmad, M. Riaz, M. Ahmad, S. Nawaz, and S. Ahmad, Mater. Lett. **62**, 3367–3369 (2008).
[16]P. W. Fowler and D. E. Manolopoulos, *The Atlas of Fullerenes* (Dover Publications, Inc., New York, 2006).
[17]P. J. Stephens, J. Chem. Phys. **52**, 3489–3516 (1970).
[18]W. R. Mason, *A Practical Guide to Magnetic Circular Dichroism Spectroscopy* (John Wiley & Sons, Inc., New Jersey, 2007).
[19]R. Bauernschmitt, R. Ahlrichs, F. H. Hennrich, and M. M. Kappes, J. Am. Chem. Soc. **120**, 5052–5059 (1998).
[20]J. P. Hare, H. W. Kroto, and R. Taylor, Chem. Phys. Lett. **177**, 394–398 (1991).
[21]Z. Gasyna, P. N. Schatz, J. P. Hare, T. J. Dennis, H. W. Kroto, R. Taylor, and D. R. M. Walton, Chem. Phys. Lett. **183**, 283–291 (1991).
[22]M. Pilch, M. Pawlikowski, and O. S. Mortensen, Chem. Phys. **172**, 277–283 (1993).
[23]F. Negri, G. Orlandi, and F. Zerbetto, Chem. Phys. Lett. **144**, 31–37 (1988).
[24]M. Pawlikowski, M. Pilch, and T. A. Keiderling, Chem. Phys. **178**, 341–348 (1993).
[25]C. N. Tam, B. L. Wang, T. A. Keiderling, and W. G. Golden, Chem. Phys. Lett. **198**, 123–127 (1992).
[26]T. Kjaergaard, P. Jorgensen, A. J. Thorvaldsen, P. Salek, and S. Coriani, J. Chem. Theory Comput. **5**, 1997–2020 (2009).
[27]M. Seth, J. Autschbach, and T. Ziegler, J. Chem. Theory Comput. **3**, 434–447 (2007).
[28]M. Seth, M. Krykunov, T. Ziegler, J. Autschbach, and A. Banerjee, J. Chem. Phys. **128**, 144105 (2008).
[29]M. Seth, M. Krykunov, T. Ziegler, and J. Autschbach, J. Chem. Phys. **128**, 234102 (2008).
[30]M. Krykunov, M. Seth, T. Ziegler, and J. Autschbach, J. Chem. Phys. **127**, 244102 (2007).
[31]H. Solheim, L. Frediani, K. Ruud, and S. Coriani, Theor. Chem. Acc. **119**, 231–244 (2008).
[32]H. Solheim, K. Ruud, S. Coriani, and P. Norman, J. Chem. Phys. **128**, 094103 (2008).
[33]DALTON2011, a molecular electronic structure program (2011), see http://www.daltonprogram.org.
[34]ADF, Vrije Universiteit, Amsterdam, 2010, see http://www.scm.com/.
[35]G. A. Peralta, M. Seth, and T. Ziegler, Inorg. Chem. **46**, 9111–9125 (2007).
[36]H. Solheim, K. Kornobis, K. Ruud, and P. M. Kozlowski, J. Phys. Chem. B **115**, 737–748 (2011).
[37]P. Štěpánek, V. Andrushchenko, K. Ruud, and P. Bouř, J. Phys. Chem. A **116**, 778–783 (2012).
[38]K. N. Semenov, N. A. Charykov, V. A. Keskinov, A. K. Piartman, A. A. Blokhin, and A. A. Kopyrin, J. Chem. Eng. Data **55**, 13–36 (2010).
[39]R. S. Ruoff, D. S. Tse, R. Malhotra, and D. C. Lorents, J. Phys. Chem. **97**, 3379–3383 (1993).
[40]See supplementary material at http://dx.doi.org/10.1063/1.4802763 for more experimental spectra and computational details including electronic transition list.
[41]A. D. Becke, Phys. Rev. A **38**, 3098–3100 (1988).
[42]J. P. Perdew, Phys. Rev. B **33**, 8822–8824 (1986).
[43]R. Ahlrichs, M. Baer, M. Haeser, H. Horn, and C. Koelmel, Chem. Phys. Lett. **162**, 165–169 (1989).
[44]M. J. G. Peach, P. Benfield, T. Helgaker, and D. J. Tozer, J. Chem. Phys. **128**, 044118 (2008).
[45]K. M. Lee, K. Yabana, and G. F. Bertsch, J. Phys. Chem. **134**, 144106 (2011).
[46]F. Ding, B. E. Van Kuiken, B. E. Eichinger, and X. Li, J. Chem. Phys. **138**, 064104 (2013).
[47]P. Štěpánek and P. Bouř, "Computation of magnetic circular dichroism by sum over states summations," J. Comput. Chem. (published online).